2B.6 RELATING TROPICAL CYCLONE RAINFALL PATTERNS TO STORM SIZE

Corene J. Matyas *
University of Florida, Gainesville, Florida

1. INTRODUCTION

During the period 1970-1999, Rappaport (2000) found that almost 60% of TC-related deaths in the U.S. were due to fresh water floods caused by heavy rainfall. To reduce this statistic, it is important to improve the accuracy of TC rainfall forecasts by examining the spatial distribution of the rain shield about the criculation center of the storm.

Previous researchers have investigated TC rainfall patterns by placing a grid over each storm and determining the rainfall amounts within each grid cell. The spatial resolution of these grid cells has ranged from 15 – 111 km^2 (Cerveny and Newman 2000; Rao and Macarthur 1994; Rodgers et al. 1994). Within each study, the same grid was utilized to analyze all of the TCs. However, utilizing a "one size fits all" grid does not allow for a relationship between a TC's size and the spatial extent of its rain shield to be established.

This study investigated whether a relationship exists between TC size and the spatial distribution of TC rainfall by utilizing sets of annular rings spaced according to each storm's size, and by investigating asymmetries in the extent of the rain shield and wind radii in each quadrant of the storm. Merrill (1984) found that TCs are largest as they migrate into subtropical latitudes where they begin to encounter sources of angular momentum such as mid-latitude troughs, and that the majority of U.S. landfalling TCs have reached their maximum size. If TC rainfall patterns are related to their size, changes in storm size prior to landfall could help forecast the location of post-landfall TC precipitation.

* *Corresponding author address:* Corene J. Matyas, University of Florida, Department of Geography, P.O. Box 117315, Gainesville, FL 32611-7315; e-mail matyas@ufl.edu

2. PROCEDURE

Base reflectivity radar returns acquired from the Department of Meteorology at Pennsylvania State University were georeferenced (Shipley 2000) and entered into a Geographic Information System (GIS) for spatial analysis. Data from neighboring stations were composited, and these point data were then interpolated into polygons that represent the rain shield. The 20 dBZ reflectivity level served as the perimeter for each polygon (Fig. 1). Additional details regarding the spatial analysis of the radar data can be found in Matyas (2005). Eleven TCs were examined at the hour of landfall (Table 1).

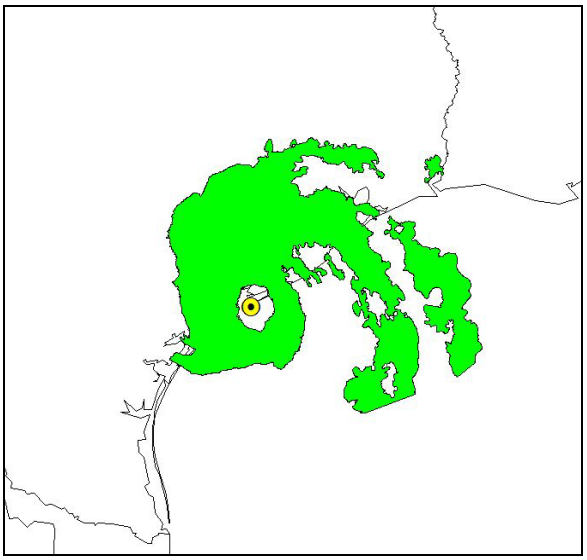

Fig.1. Rain shield of Hurricane Claudette (2003) at the time of landfall. Yellow circle represents the circulation center of the TC.

The wind radii in each quadrant, as well as the coordinates of the storm circulation centers and intensity data, were acquired from the National Hurricane Center website (www.nhc.noaa.gov). Storm size was calculated by averaging the radius that gale force winds

(RGW) extended out from the center of the storm in all four quadrants. In the same manner, size was also determined for each of eight TCs using the averaged radius of tropical storm-force winds (RTW), and for the six hurricanes using the averaged radius of hurricane-force winds (RHW) (Table 1) (Kimball and Mulekar 2004).

Table 1. Average radius (km) of gale-, tropical storm-, and hurricane-force winds, and the outer edge of the rain shield for the eleven TCs in the study.

TC	RGW	RTW	RHW	Rain Shield
Bonnie (1998)	247	179	128	188
Charley (1998)	197	-	-	134
Georges (1998)	225	137	51	238
Hermine (1998)	58	-	-	83
Bret (1999)	194	77	44	139
Dennis (1999)	185	31	-	234
Irene (1999)	220	81	30	189
Gordon (2000)	135	61	-	219
Helene (2000)	91	-	-	180
Claudette (2003)	192	70	23	198
Isabel (2003)	405	211	153	392

Within the GIS, sets of annular rings were created by buffering the circulation center of each storm (Fig. 2). Each set of rings was used to clip the rain shield polygons, and the areal coverage of the rain shield within each pair of rings was determined. Because each of these regions encloses a different-sized area, the percentage of region that is occupied by the rain shield was calculated to facilitate the comparison of all regions.

As a control to simulate the results of previous researchers, all TCs were clipped by a set of annular rings spaced in 50 km increments. Each TC was then clipped using a set of annular rings based on its RGW in one-half increments. Table 1 shows the TCs whose rain shields were also clipped using annular grids sized according to their RTW and RHW.

The calculation of eight additional variables assessed the areal extent and asymmetrical distribution of the rain shield as a whole. As the wind radii can vary widely across all four quadrants, it is reasonable to assume that the spatial extent of the rain shield should also differ among the quadrants. Thus, the distance from the circulation center to the outer edge of the rain shield was recorded for each quadrant. These data were averaged to calculate the rain shield extent listed in Table 1. Summing the areas of all polygons that comprise the rain shield yielded the total areal coverage (Tarea) of the rain shield. The geographical center, or centroid, of the rain shield was determined, and the distance and bearing of this point relative to the circulation center was calculated as a measure of symmetry. The major-to-minor axis ratio (MMR), or elongation, of the rain shield was calculated by measuring the longest (major) axis that passes through the centroid, measuring the length of the minor axis, which is perpendicular to the major axis, and then dividing the length of the minor by length of the major axis. The degree to which the rain shield encloses the circulation center, or the rain shield arc length (RSAL) is also noted as a third measure of rain shield symmetry (Matyas 2006).

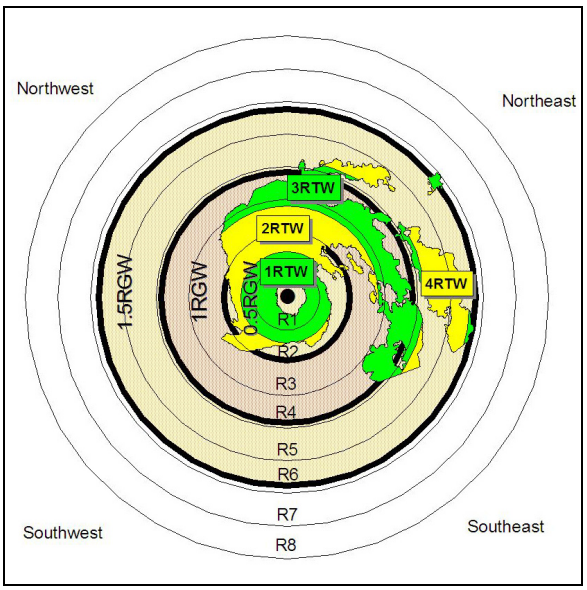

Fig. 2. Clipping the rain shield of Claudette shown in Fig 1 by three sets of annular rings: 1) 50 km-spaced set used to clip all storms (gray rings whose regions are labeled R1-R8); 2) radius of gale-force winds (alternating light and dark orange-shaded regions); and 3) radius of tropical storm-force winds (alternating green and yellow regions of the rain shield).

Pearson correlation coefficients were calculated for all data collected. These values determined which set of annular rings best correlated to the overall shape of the storm, and which variables best correlated to the asymmetrical distribution of the rain shield in each quadrant.

3. RESULTS

3.1 Comparisons using storm-averaged wind and rain shield spatial extents

Comparing the average RGW to the average radius of the rain shield for each TC (Table 1) shows that hurricane rain shields are mostly contained within the RGW, whereas tropical storm rain shields tend to extend beyond their RGW. The average extent of the rain shield was inside the RGW of four of the hurricanes, and the rain shield only averaged six and thirteen kilometers outwards of the RGW in the other two hurricanes. In contrast, the rain shield extended 25-89 km outside the RGW of the tropical storms examined in this study. These results imply that storm size as measured by the RGW may be a useful measurement for determining the spatial extent of the rain shield for hurricanes, but may not adequately represent the outermost edge of a tropical storm rain shield.

Fig. 3 shows that the percent of rain shield coverage within each annular ring region differs according to storm intensity. Due to relatively fast tangential winds, moisture circulates all the way around the inner core of a hurricane, so that regions R1, R2, and R3 are at least 30% covered by the rain shield (Fig. 3). Tropical storms, with the exception of Dennis as it was approaching hurricane intensity at landfall, had less inner core rain shield coverage.

Differences in rain shield coverage according to storm intensity were also evident when using the size-based annular rings. When using the RGW to section the storms, hurricane rain shields were all contained within 1.5 times the RGW, while tropical storm rain shields extended out to 5RGW (Fig. 4). The two non-hurricanes that had measurable tropical storm-force wind radii had rain shields which extended outwards of 10 times their RTW, while the hurricane rain shields were contained within six times their RTW (Fig. 5). Differences in rain shield distribution were evident even within the hurricanes. The two category one hurricanes had rain shields that extended outwards of eight times their RHW, while the category two and three hurricanes had rain shields within this distance (Fig. 6). These results suggest that more intense TCs have most of their rain shields located within the inner core of the storm, yielding a rain shield with a circular shape. The correlation between the maximum sustained wind speed of each storm at landfall and its MMR value is 0.913, which supports this finding as it indicates that storm elongation is highly correlated to intensity.

The 50 km annular rings yielded the most information about the spatial characteristics of the rain shields themselves because they were correlated to both the shape and the areal coverage of the rain shield (Table 2). The three innermost annular rings (R1, R2, R3) were highly correlated to the shape of the rain shield, meaning that a greater coverage of rain shield within these regions corresponded to a more circular shape, a centroid located closer to the circulation center, and a circulation center that was enclosed by the rain shield. Shields that extend over a larger area have more coverage 150-300 km from the storm center.

Table 2. Pearson correlation coefficients for annular rings and storm shape variables. Values shown are statistically significant at $\alpha = 0.05$. Values in bold italics are significant at $\alpha = 0.01$.

Ring	Tarea	MMR	Dist	RSAL
R1	-	***0.866***	***-0.758***	***0.860***
R2	-	***0.936***	***-0.819***	***0.939***
R3	-	***0.826***	***-0.741***	0.770
R4	***0.860***	-	-	-
R5	***0.878***	-	-	-
R6	***0.871***	-	-	-
0.5RGW	-	***0.913***	***-0.795***	***0.932***
1RGW	-	0.706	-0.626	0.723
1RTW	-	0.797	-	***0.895***
1RHW	-	***0.931***	-	-

Similar correlations can be found when utilizing increments of the RGW to section the rain shields. TCs having a relatively "full" 0.5RGW region are more symmetrical in shape

(Table 2). The strength of this finding for both the 50 km and RGW sets of annular rings suggests that processes affecting the inner core of the storm have the most impact on the spatial extent of the entire rain shield. Removing tropical storms from the analysis strengthened the correlation values between the RGW data and the variables characterizing storm shape. These findings again suggest that the size of the storm as measured by the RGW is related to the spatial extent of the rain shield for hurricanes. However, the asymmetrical structure of tropical storms does not allow for the RGW to have a strong relationship with the spatial extent of the rain shield.

3.2 Comparisons of wind radii and rain shield extent by quadrant

As TCs migrate into higher latitudes, their circulations become increasingly susceptible to the influences of middle latitude weather systems, often resulting in an asymmetrically-shaped rain shield. Atallah and Bosart (2003) describe how a TC's rain shield can increase on its left side after an extratropical transition is completed. In other cases, dry air infiltration from continental air masses can help reduce the spatial extent of the rain shield on the western side of the storm, as described by Bluestein and Hazen (1989).

Fig. 7 illustrates the asymmetrical distribution of the spatial extent of the TC rain shields and wind radii in each quadrant. Many TC rain shields, particularly tropical storms, exceed the extent of their RGW in the northeast quadrant. The rain shield and wind radii extents appear to be more closely related in spatial proximity in the northwest quadrant of each storm. To determine which measure of storm size best relates to the rain shield coverage in each quadrant of the storm, correlation coefficients were calculated for the distance from the storm center to the rain shield's outer edge in each quadrant, and the radius of hurricane-, tropical storm-, and gale-force winds for each quadrant (Table 3).

The strong correlations between the rain shield and all wind radii in the northwest and southwest quadrants (Table 3) suggests that the synoptic environment is controlling storm structure on the western side of the circulation center. The RHW, RTW, and RGW winds in both the northwest and southwest quadrants have significant correlations to the extent to the rain shield in the northwest and southwest quadrants. All eight of these variables are also highly correlated to the total areal coverage of the rain shield (Table 4), again suggesting that atmospheric conditions are affecting the storm structure to the west of the storm center.

Table 3. Pearson correlation coefficients for the wind radii in each quadrant and storm shape variables. Values shown are statistically significant at α = 0.05. Values in italics are significant at α = 0.01.

Quadrant Wind Radii	Rain Shield Extent Northwest	Rain Shield Extent Southwest
RHW NW	0.610	***0.816***
RHW SW	0.615	***0.796***
RTW NW	***0.809***	***0.911***
RTW SW	0.630	***0.821***
RGW NW	***0.864***	***0.740***
RGW SW	***0.833***	***0.863***

Table 4. Pearson correlation coefficients for the wind radii in each quadrant and storm shape variables. Values shown are statistically significant at α = 0.05. Values in italics are significant at α = 0.01.

Quadrant Wind Radii	Tarea	EL	Dist	RSAL
RTW SE	-	0.701	***-0.749***	-
RTW NE	-	***0.865***	***-0.667***	***0.775***
RTW NW	***0.854***	***-***	-	0.680
RTW SW	***0.757***	***-***	-	-
RGW SE	***-***	***0.773***	-	0.644
RGW NW	***0.812***	-	-	-
RGW SW	***0.883***	-	-	0.603

That the extent of the rain shield on the right side of the storm was not highly correlated to any of the wind radii on the east side suggests that other factors, such as the increased friction at the time of landfall, may be enhancing the

spatial extent of the rain shield in this area. Ten out of eleven of the storms in this study were tracking westward or northward at the time of landfall. This means that the eastern half of the storm was still able to gain moisture from the ocean surface, allowing the rain shield in the eastern quadrants of the storm to develop beyond the RGW. The finding that rain shield elongation and the distance of the centroid from the storm center are highly correlated to the RTW on the eastern side of the storm (Table 4), supports the suggestion that the eastern half of the storm is controlled by its interaction with the ocean surface at the time of landfall.

4. CONCLUSIONS AND FUTURE RESEARCH

The results of this study indicate that the spatial extent of hurricane rain shields are closely related to their radius of gale-force winds. Hurricanes have more of their rain shield located within their inner core than tropical storms, and thus the amount of precipitation located both within 150 km and within the RGW is indicative of the elongation and symmetry of the rain shield itself. Larger TCs have more of their rain shield located in the region that is 200-300 km outwards from the circulation center.

Due to the asymmetrical structure of tropical storms, a larger portion of their rain shields are located outside of the 150 km radius and outside the RGW, particularly in the northeast quadrant of the storm, as compared to hurricanes. Thus, tropical storm size as measured by the RGW is not as well correlated to the spatial extent of the rain shield as it was for hurricanes.

When examining the asymmetrical distribution of the rain shields's outer extent by quadrant, strong correlations were found between the wind radii and rain shield extent on the western side of the storm, as well as the total areal coverage of the rain shield. The fact that these high correlation values existed only on the west side of the TCs, while the elongation and polygon centroid distances were only correlated to the wind radii on the eastern side of the storm suggests that the controls of storm structure may differ between the two sides during landfall. The western (eastern) side may be more strongly influenced by the atmosphere (ocean surface).

Future work will examine additional TCs to further investigate the results of this study. The ability to spatially analyze radar data within a GIS (Ansari and Del Greco 2005) will allow many additional TCs to be analyzed. TCs will also be examined in the hours prior to and just after landfall to determine if changes in the spatial extent of the rain shield are correlated with changes in storm size throughout the landfall process.

5. REFERENCES

Ansari, S., and S. Del Greco, 2005: GIS tools for visualization and analysis of NEXRAD radar (WSR-88D) archived data at the National Climatic Data Center. *21st International Conference on Interactive Information Processing Systems (IIPS) for Meteorology, Oceanography, and Hydrology*, San Diego, CA, AMS.

Atallah, E. H., and L. R. Bosart, 2003: The extratropical transition and precipitation distribution of Hurricane Floyd (1999). *Mon. Weather Rev.*, **131,** 1063-1081.

Bluestein, H. B., and D. S. Hazen, 1989: Doppler-radar analysis of a tropical cyclone over land - Hurricane Alicia (1983) in Oklahoma. *Mon. Weather Rev.*, **117,** 2594-2611.

Cerveny, R. S., and L. E. Newman, 2000: Climatological relationships between tropical cyclones and rainfall. *Mon. Weather Rev.*, **128,** 3329-3336.

Kimball, S. K., and M. S. Mulekar, 2004: A 15-year climatology of North Atlantic tropical cyclones. Part I: Size parameters. *J. Clim.*, **17,** 3555-3575.

Matyas, C. J., 2005: Using geographical information systems for the spatial analysis of base reflectivity radar data and applications to the study of tropical cyclone precipitation patterns. *15th Conference on Applied Climatology, American Meteorological Society*, Savannah, GA, American Meteorological Society.

——, 2006: Calculating Shape Metrics to Quantify the Spatial Patterns of Tropical Cyclone Rain Shields. *submitted to Applied Geography February 2006.*

Merrill, R. T., 1984: A comparison of large and small tropical cyclones. *Mon. Weather Rev.*, **112,** 1408 - 1418.

Rao, G. V., and P. D. Macarthur, 1994: The SSM/I estimated rainfall amounts of tropical cyclones and their potential in predicting the cyclone intensity changes. *Mon. Weather Rev.*, **122,** 1568-1574.

Rappaport, E. N., 2000: Loss of life in the United States associated with recent Atlantic tropical cyclones. *Bull. Amer. Meteorol. Soc.*, **81,** 2065-2073.

Rodgers, E. B., J. J. Baik, and H. F. Pierce, 1994: The environmental influence on tropical cyclone precipitation. *J. Appl. Meteorol.*, **33,** 573-593.

Shipley, S. T., http://geog.gmu.edu/projects/wxproject: NEX2SHP.exe utility courtesy of George Mason University, Department of Geography

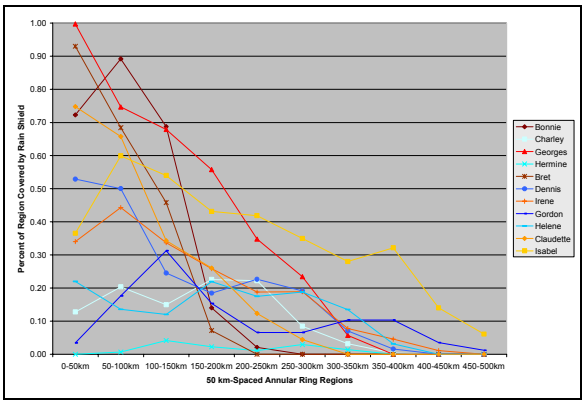

Fig. 3 Percent of area covered by the rain shield with each region that is bounded by annular rings spaced in 50 km increments. Hurricanes are designated by the red color group, while tropical storms are in blue.

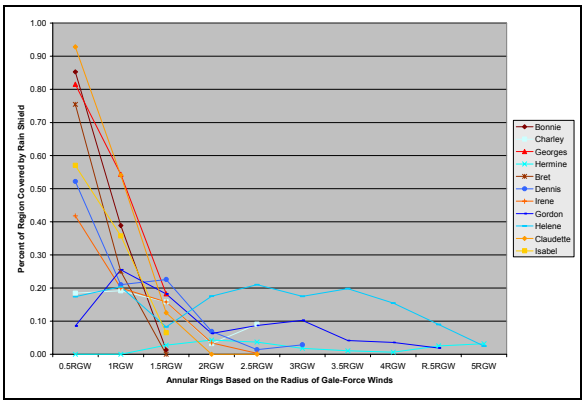

Fig. 4 Percent of area covered by the rain shield with each region that is bounded by increments of one half of the radius of gale-force winds. Hurricanes are designated by the red color group, while tropical storms are in blue.

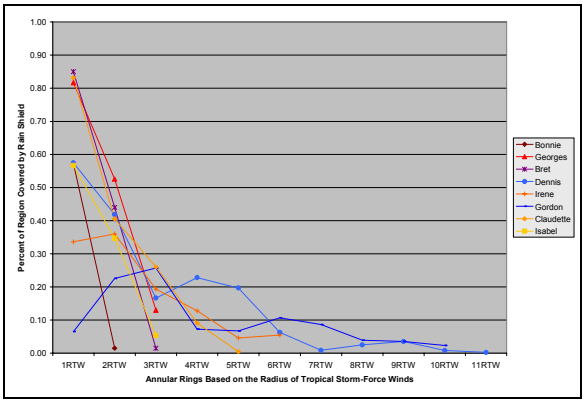

Fig. 5 Percent of area covered by the rain shield with each region that is bounded by increments of the radius of tropical storm-force winds. Hurricanes are designated by the red color group, while tropical storms are in blue.

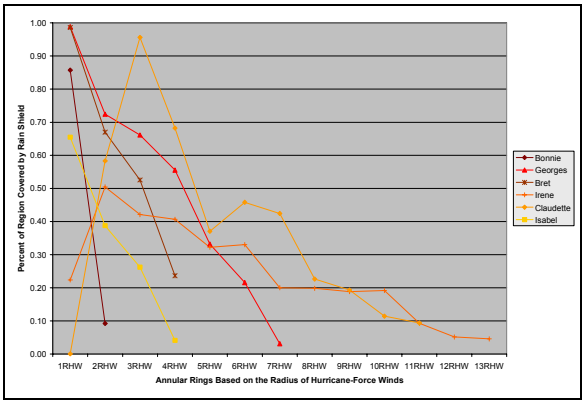

Fig. 6 Percent of area covered by the rain shield within each region that is bounded by increments of the radius of hurricane force winds for each hurricane in the study.

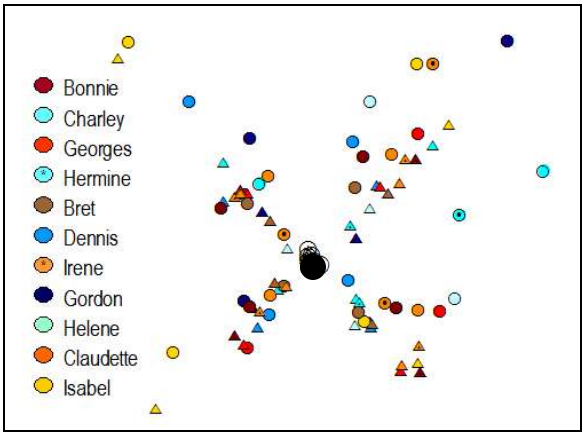

Fig. 7 Overlay of the wind radii and outer edge of the rain shields for all 11 TCs. The extent of the rain shield in each quadrant is marked with a circle. Triangles represent the RGW. Hurricanes are in the red color group, while tropical storms are in the blue color group. The center of circulation is in the middle of the image, and the top of the image is north.